Effect of Nanofiller Content and Confined Crystallization on the Microphase Separation Kinetics of Polyurethane Nanocomposites

Iman Sahebi Jouibari, Vahid Haddadi-Asl, Mohammad Masoud Mirhosseini
Department of Polymer Engineering and Color Technology, Amirkabir University of Technology (Tehran Polytechnic), Tehran, Iran

The multiwalled carbon nanotubes (MWCNTs), Closite 30B nanoplates (CBNPs), and halloysite nanotubes (HNTs) reinforced thermoplastic polyurethane (TPU) nanocomposites were prepared via melt compounding method and evaluated with several techniques including microscopy, spectroscopy, thermal, and rheological analyses. Degree of microphase separation and nucleation efficiency of nanocomposites were calculated. Results showed that at 0.1 wt% nanofiller content, the nanocomposites possess the fastest microphase separation kinetics and the highest degree of microphase separation. Avrami equation was used to analyze the crystallization behavior of samples. Based on the rheological and microscopy analyses, existence of microphase separation above the percolation threshold was observed for annealed samples. Finally, competition between reagglomeration of nanofillers and formation of microphase separated domains above the percolation threshold at various nanofiller contents, shear rates and temperatures was discussed. POLYM. COMPOS., 00:000–000, 2018. © 2018 Society of Plastics Engineers

INTRODUCTION

Thermoplastic polyurethane (TPU), an AB-type block copolymer consisting of hard segments (A) and soft segments (B) arranged in a linear block structure, has been used in many potential applications like artificial heart diaphragms, sporting goods, medical tubing, healthcare mattresses, wire and cable coatings, and so forth [1, 2]. Microphase separation occurs due to the thermodynamic incompatibility of the soft and hard segments at low temperatures. The soft segment is widely considered to be the continuous phase in which the hard domains are randomly distributed. It is well understood that hard segment-rich domain acts as a physical crosslink and its outstanding mechanical properties are shown in TPU. The engineering properties of TPU are intensely dependent on the degree of the microphase separation and morphology of the microphase separated domains [3, 4]. Numerous factors like chemical structure of ingredients, hard/soft segment ratio, crystallizability of hard and soft segments, polymerization procedure, inherent miscibility of hard and soft segments, segmental length, hard segment mobility and flexibility, process parameters and presence of nanofillers affect the morphology and microphase separation of TPU [5–7]. Due to the extremely high surface area in nanocomposites, an improvement of the mechanical, barrier and thermo-mechanical properties, and conductivity can be achieved at low filler contents which marks the main advantage of these materials over the microphase reinforced composites (less than 5 wt%) [8–10]. Crystallization behavior of polymer such as nucleation rate, crystallite size, crystallization temperature, and rate of crystal formation are altered by the presence of nanofillers [11, 12]. Most of the relative crystallinity analyses are based on the Avrami equation which can describe the kinetics of polymer crystallization. For instance, isothermal crystallization of nanocomposites composed of multiwalled carbon nanotubes (MWCNTs) and graphene dispersed in hot melt adhesive polyurethane has been studied by Landa et al. [13]. They have shown that the exponent of the Avrami equation (n) decreases from $n = 3$ for neat polyurethane to $n = 2$ for both nanocomposites indicating change in crystals morphology of the samples. When the effect of nanofillers is studied on the phase separation and crystallization of polymer nanocomposites, physiochemical characteristics of the nanofillers like particle size, aspect ratio, shape, chemical nature, concentrations and their interaction with polymer chains should be taken into account [14–16]. Only minor amounts of nanofillers added into semicrystalline polymers can accelerate nucleation rate of polymers. The study of CNTs/polypropylene composites by Xu and Wang revealed that crystallization rates were enhanced when CNTs content was below the percolation threshold, while the crystallization rates did not change noticeably

Correspondence to: haddadi@aut.ac.ir
DOI 10.1002/pc.24717
Published online in Wiley Online Library (wileyonlinelibrary.com).

beyond the critical gelation concentration due to formation of CNTs network [17]. The effects of acid oxidized-MWCNTs with different aspect ratios on the crystallization kinetics of polylactide nanocomposite have been studied by Xu et al. [18]. They have reported that nanotubes with smaller aspect ratios due to fewer sidewall carboxyl groups on their surfaces enhance nucleation rate for polylactide spherulites much more than those with larger aspect ratios. In addition, the MWCNT concentrations pose different effects on polylactide crystallization when MWCNT concentration is below or above the percolation value. When nanofiller concentrations are increased in the nanocomposite, the distance between intimate nanofillers or aggregates is decreased and therefore prevents polymer crystallization because of steric hindrance. The interest in confined crystallization has greatly increased with the growth of nanocomposites. Spatial restrictions on polymer chains can be introduced by restricting them to the limited space between nanofillers. The impact of geometric confinement on the crystallization behaviors of nanocomposites intensely depends on the type of nanofillers and polymer matrix [19–21]. In addition, it has been shown that the reagglomeration of nanofillers and reconstruction of the filler network affect the crystallization and phase separation of polymer nanocomposites [22, 23]. Compared with homopolymers, block copolymers like TPUs have a complex crystallization and phase separation behavior due to the coexistence of nanofillers and microphase separated domains. In TPU nanocomposites, competition between reagglomeration of nanofillers and formation of microphase separated domains would be accounted. Hence, the goal of this work is to investigate the effect of nanofiller content and confinement on the microphase separation kinetics of TPUs reinforced with MWCNTs, CBNPs and HNTs. These nanofillers have a different size, aspect ratio, shape and chemical nature, and consequently their interaction with polymer chains would be different. To this end, first, TPUs based on PTMG, MDI, and BDO were synthesized. Thereafter, TPU nanocomposites were prepared by melt processing and evaluated by many techniques including Fourier transform infrared (FTIR) spectroscopy, field emission scanning electron microscopy (FESEM), dynamic mechanical–thermal analysis (DMTA), differential scanning calorimetry (DSC) thermograms, and rheometric mechanical spectrometer (RMS).

MATERIALS AND METHODS

Materials

Poly(tetramethylene ether) glycol (PTMG) with functionality of 2 and number–average molecular weight of 2,000 (g/mol), 4,4′-Diphenylmethane diisocyanate (MDI), 1,4-butanediol (BDO) and halloysite nanotubes with inner diameter of 30–70 nm, pore volume of 1.26-1.34 mL/g, and specific surface of 64 m^2/g were purchased from Sigma–Aldrich. Organiclay modified clay Closite 30B (CEC: 90 meq/100 g), were obtained from southern Clay product. The multi-wall carbon nanotubes, Nanocyl 7,000, with average diameter of 9.5 nm, average length of 1.5 μm, and purity of 90% was supplied by Nanocyl (Belgium). *N*,*N*-Dimethylacetamide (DMAC) was obtained from Merck. All reagents were used as received without any further purification.

Synthesis of TPU

TPU was synthesized by two-step solution polymerization method. Polymerization was carried out into a two-necked round-bottomed flask equipped with a vacuum inlet tube and a raw material entrance. The reaction assembly was placed in a heating oil bath. Prior to mixing, PTMG, MDI, and BDO were dried in a vacuum oven at 80°C for 3 h to ensure residual moisture removal. For polyurethane synthesis, the molar ratio of PTMG, MDI, and BDO were determined to be 1, 3 and 2, respectively. 30 g PTMG with 45 mL DMAC was added to the flask. Later on, 11.6 g MDI was added to the content and reacted with polyol for 3 h at 75–85°C under continuous stirring to render a macro diisocyanate prepolymer. In the chain extension step, 2.74 g BDO was added to the prepolymer. During this step, the viscosity of polyurethane is slowly increased due to the ongoing chain-extension reaction. After 3 h reaction, the obtained viscous liquid was poured into a silicone mold and placed in an oven at 85°C for 24 h. Finally, all samples were removed from the mold and stored at ambient temperature.

TPU Nanocomposites Preparation

Nanocomposites were prepared via melt compounding method. To this end, TPU and varying content of CBNPs, HNTs and MWNTs (gamut from 0.05 wt% to 5 wt%) were compounded with a laboratory internal mixer (Braebender Plasticorder W50). Processing parameters, i.e., temperature and rotating speed were optimized as 210°C and 100 rpm, respectively. Melt-compounding was carried on for 18min for nanocomposite comprising the CBNPs and 15 min for nanocomposites containing the MWNTs and HNTs. Prior to mixing; TPUs were dried in a vacuum oven at 140°C for 12 h to ensure residual moisture removal.

Characterization

Fourier transform infrared (FTIR) spectra were recorded on a Bruker spectrophotometer within a range of 500–4400 cm^{-1} using a resolution of 4 cm^{-1}. The samples were prepared on a KBr pellet in vacuum desiccators under a pressure of 0.01 torr.

The morphology of samples was determined by field emission scanning electron microscopy (FESEM) (Hitachi S4160) using 30 kV accelerating voltage. The samples

 DOI 10.1002/pc

were coated with gold using a sputter coater before FESEM imaging.

Differential scanning calorimetry (DSC) experiments were conducted with a Flash DSC 1 of Mettler-Toledo, in order to evaluate the thermal properties of the nanocomposites. The experiments were conducted at a constant heating rate of 10°C/min on samples (15–20 mg) packed in aluminum pans under nitrogen flow.

Dynamic mechanical properties of nanocomposites were measured using dynamic mechanical thermal analyzer Diamond DMA Perkin Elmer in the tensile mode at frequency of 1 Hz on molded samples (20*11*1 mm). The test was carried out at a frequency of 1 Hz, static force of 0.1 N, and the temperature range −100 to 150°C and a scan rate of 5°C/min under nitrogen atmosphere.

To measure the linear viscoelastic responses of neat TPU and the nanocomposites, a Rheometrics mechanical spectrometer (Paar Physica UDS200), equipped with a parallel plate fixture (25 mm diameter and a constant gap of 1 mm), was employed. The neat TPU was heated for 15 min and 5 min for TPU nanocomposites in order to erase thermal history, residual stress, and hard domains in melting temperature. The neat TPU and the nanocomposites were cooled rapidly to the annealing temperature. This cooling process usually took 2 min for 50–70°C drops in temperature. Then the storage modulus and the loss modulus (G', G'') of the samples were measured by a time sweep experiment in order to study the microphase separation and hard domain aggregation, at an annealing temperature for 2 h. In order to investigate the effect of shear flow on microphase separation kinetics, time sweep experiment was conducted at various preshear rates, ranging from 5 to 30 s^{-1}, before starting time sweep test at annealing temperature. In order to determine microphase separation temperature, the cooling process was carried out at the rate of 10°C/min (same as the rate of DSC experiments) for neat TPU and from melting temperature (210°C) to near the hard segments glass transition temperature (120°C) for nanocomposites.

RESULTS AND DISCUSSION

It is well accepted that the rheology is one of the most sensitive tools to study the dynamic of chains and the formation of three-dimensional elastic networks. In addition to the DSC test, time sweep test was used to determine the nucleation efficiency of the nanocomposites. Based on the RMS and DSC analyses, nucleation efficiency of the nanocomposites is discerned and data are summarized in Fig. 1. Here, nanofillers act as the initiative for the process of nucleation. By self-organization or self-assembly of polymer chains, a new phase or structure could form which is called nucleation. The nucleation efficiency (NE) of the nanocomposites is calculated using the following equation [11, 24]:

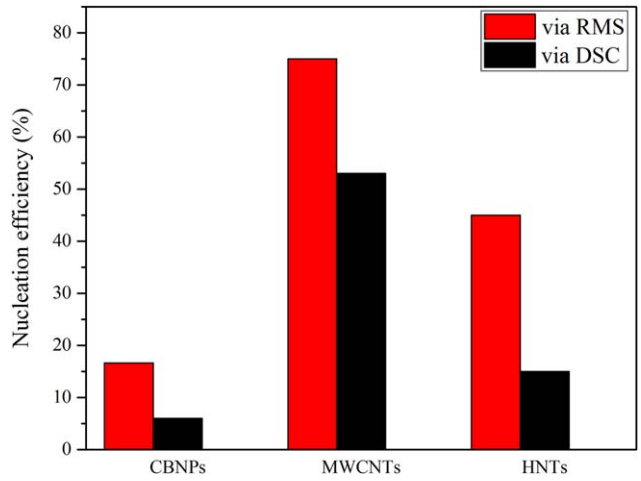

FIG. 1. Nucleation efficiency of nanocomposites based on the RMS and DSC analyses. [Color figure can be viewed at wileyonlinelibrary.com]

$$\mathrm{NE}=\frac{(T_{\mathrm{CNA}}-T_{\mathrm{CP}})}{(T_{\mathrm{CMP}}-T_{\mathrm{CP}})} \tag{1}$$

where in the DSC analysis, T_{CNA} is the peak crystallization temperature of the polymer nanocomposite with the nucleating agent. T_{CP} is the peak crystallization temperature of the neat polymer (without any nucleating agent and with a standard thermal history), and T_{CMP} is the maximum crystallization temperature of the ideally self-nucleated neat polymer. In the RMS analysis, T_{CNA} is the temperature which after 2,000 s TPU nanocomposites could form cross time (collision of storage and loss modules). T_{CMP} is the maximum temperature in which increment of the storage modules (hard domains formation) could be seen, T_{CP} is the minimum nucleation temperature of neat TPUs. As seen from Fig. 1, the typical values of the NE are between 15% and 75% for RMS analysis whereas the aforesaid values are in the range of 5 to 55% for DSC analysis. It is observed that the maximum of NE belongs to the MWCNTs; because the MWCNTs have the outstanding ability to absorb hard segments via noncovalent π-π interactions and thereby they can act as effective nucleating agents to crystallize the TPU hard segments [25].

The dissipation factor (tanδ) of the soft segments is given as function of temperature in Fig. 2. The glass transition temperature (T_g) of the soft segments is indicated by maximum of the curves. Figure 2 clearly shows that the glass transition temperature of the soft segments is located at the negative temperatures. At this temperature, soft segments can easily move due to the adequate thermal energy. Since TPUs are composed of polar hard segments and much less polar soft segments, final structure is formed by microphase separated assembly and mixture of hard and soft segments. As the PTMG used as a polyol has a very low polarity, it is expected that degree of microphase separation would be noticeable due to the high thermodynamic incompatibility of the soft and hard

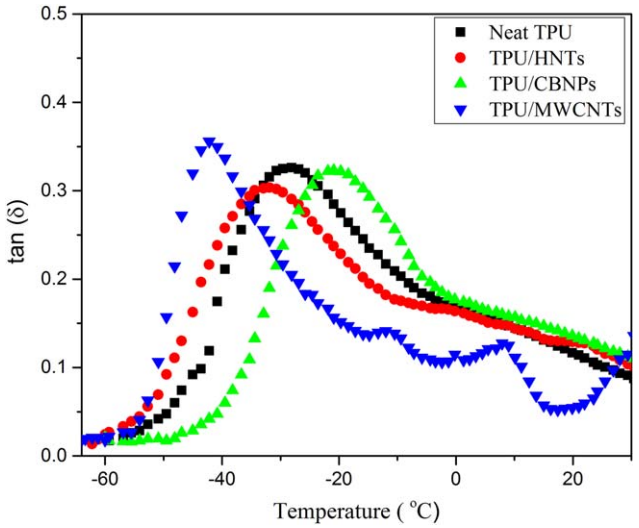

FIG. 2. tan (δ) of the soft segments as function of temperature. [Color figure can be viewed at wileyonlinelibrary.com]

segments. It is well known that difference in chemical nature of the nanofillers leads to their various interactions with soft and hard segments of polyurethane. The MWCNTs and HNTs have more affinity to interact with hard segments than soft ones, thus the soft segments have more freedom to move. As seen from Fig. 2, these nanocomposites have lower soft segments T_g comparing the ones with CBNPs. CBNPs have no affinity to interact with the hard segments. They are embedded into the soft segments and prevent their mobility. Therefore, the presence of the CBNPs require more thermal energy for segmental motion and consequently the tanδ peak shifts toward the higher temperatures.

FTIR analysis has been widely used to study microphase separation of polyurethanes. There is a wide range of molecular interactions like hydrogen bonding, dipole–dipole, and induced dipole–dipole interactions between hard segments that strongly affect the microphase separation. Based on the two absorption peaks located at 3,445 and 3,348 cm^{-1} corresponding to the free and hydrogen-bonded N—H stretching, respectively, the degree of microphase separation (DPS) can be calculated by means of the next equations [26]:

$$\mathrm{DPS}=\frac{\mathrm{NH_{bonded}}}{\mathrm{NH_{bonded}}+\mathrm{NH_{free}}} \tag{2}$$

where NH_{bonded} is the intensity of the characteristic absorbance at 3,348 cm^{-1} and NH_{free} is that at 3,445 cm^{-1}. Based on the FTIR spectra, the DPS of the samples are calculated (Table 1). Results from Table 1 show that degree of microphase separation of the samples containing 0.1 wt% nanofiller is higher than the nanocomposites above the percolation threshold. Segmental incompatibility in the polyurethane increases by adding MWCNTs. The higher the affinity to interact with the hard segments, the higher DPS is obtained. The DPS of the CBNPs and HNTs

TABLE 1. DPS of the samples.

Sample	DPS (%)
Neat TPU	74
TPU/MWCNTs (0.1 wt%)	78
TPU/MWCNTs (1 wt%)	71
TPU/HNTs (0.1 wt%)	70
TPU/HNTs (2 wt%)	69
TPU/CBNPs (0.1 wt%)	72
TPU/CBNPs (5 wt%)	67

nanocomposites is reduced due to obstructive effect of nanofillers and accordingly the hydrogen bonds are diminished, with respect to the neat TPU. We found that the DPS of TPUs filled with the optimum content of MWCNTs, CBNPs, and HNTs was increased 9.85%, 7.47%, and 1.44%, respectively, compared to the nanocomposites above the percolation threshold.

Crystallinity analyses are based on the Avrami equation as shown by the following equation [13]:

$$G'(t)=G'_0+G'_\infty(1-\exp(-kt^n))^2 \tag{3}$$

where G'_0 is the shear modulus before crystallization onset, G'_∞, the modulus when crystallization is completed (crystalline volume fraction $\emptyset = 1$) and k and n are the fitting parameters of the Avrami equation, $\emptyset=(1\text{-}\exp(\text{-}Kt^n))$. Furthermore, the half crystallization time ($t_{1/2}$) can be estimated:

$$t_{1/2}=\left(\frac{\ln 2}{k}\right)^{1/n} \tag{4}$$

The corresponding values of the Avrami parameters obtained by rheological results are presented in Table 2. It is noteworthy that the Avrami parameters presented in Table 2 should be compared with the samples containing nanofiller concentrations above and below the percolation threshold separately. Once the nanofillers are incorporated into TPU matrix, half crystallization time decreases strongly compared with the neat TPU. A decrease of $t_{1/2}$ and k is observed in general by adding the nanofillers. This behavior does not correspond to microphase separation kinetics for nanocomposites above the percolation threshold and it is related to formation of nanofillers networks. It is

TABLE 2. Values of the Avrami parameters, K, n, and the half crystallization time, of the samples.

Sample	n	k(s^{-1})	$t_{1/2}$(s)
Neat TPU	1.45	4.8e-06	3.5e+03
TPU/MWCNTs (0.1 wt%)	1.58	1.0e-03	62.6916
TPU/MWCNTs (1 wt%)	1.11	0.02	23
TPU/HNTs (0.1 wt%)	1.26	6.3e-05	1.5e+03
TPU/HNTs (2 wt%)	1.08	0.0042	112.7
TPU/CBNPs (0.1 wt%)	1.35	4.1e-05	2.0e+03
TPU/CBNPs (5 wt%)	1.03	0.032	214.5

DOI 10.1002/pc

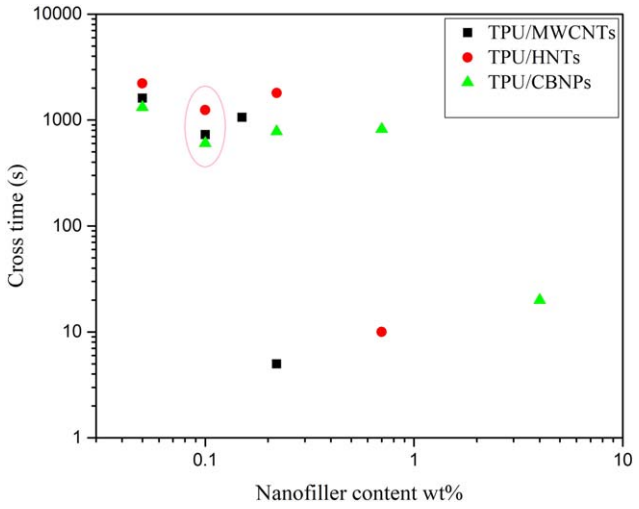

FIG. 3. Cross time as a function of nanofiller content. [Color figure can be viewed at wileyonlinelibrary.com]

clear from Table 2 that the MWCNTs have the most effect on the crystallization kinetics.

Figure 3 shows cross time as a function of nanofiller content. It is obvious from Fig. 3 that at 0.1 wt% nanofiller content, the three samples have the fastest microphase separation kinetics. Moreover, at percolation threshold low cross times are discerned which can be related to formation of nanofillers networks and not to microphase separation. To clarify that why the fastest microphase separation kinetics is observed at the specific nanofillers content for all samples, number of nanofillers and hard segments, total surface area of nanofillers, required surface area and excess required nanofillers have been summarized in Table 3. According to the results, it is revealed that for nucleation of all hard segments, excess amount of nanofillers are required. In the following, attempts are made to explain why the fastest microphase separation kinetics occurs at 0.1 wt% nanofillers content. The addition of nanofillers more than the specific value causes to confine the mobility of the polymer chains. The numbers of surface area are sufficient for nucleation and the other hard segments do not require nuclei for nucleation. Because dynamic of chains is reduced in the presence of the specific nanofiller amount and the hard segments can act as the initiative for the process of nucleation. Some residual hard segments participate in secondary crystallization process. All hard segments do not need to participate in microphase separation process.

Figure 4 schematically illustrates microphase separation of TPU nanocomposites containing low and high MWCNTs content. The presence of microphase separated domains near the nanotube (Fig. 4a) indicates that MWCNTs can act as effective nucleating agents to crystallize the TPU hard segments. Nevertheless, once the nanotube content is enhanced, the distance between close MWCNTs is decreased and therefore prevents the hard segment microphase separation. As seen in Fig. 4b, the MWCNTs confine the mobility of TPU chains and accordingly their ability to assemble each other is reduced.

FESEM images of the neat TPU, TPU/CBNPs, TPU/HNTs, and TPU/MWCNTs are presented in Fig. 5a–d. Cylindrical domains assigned to microphase separation of the hard and soft segments caused by thermodynamic incompatibility between polar hard segments and much less polar soft segments are revealed in Fig. 5a. Since the samples are quenched, it is obvious from Fig. 5b-d that above percolation threshold, agglomerations of nanofillers confine the mobility and microphase separation of the hard segments. This causes that microphase separated domains do not exist in the aforesaid figures. The theoretical model proposed by Lipatov gave a quantitative relation for calculating thickness of the layers between two nanofillers as [27]

$$\delta = \frac{V}{(S_{sp} G_f)} \tag{5}$$

where V is the volume of the TPU, S_{sp} is the specific surface of a nanofiller, and G_f is the mass of the nanofillers. Thickness of the layers between two nanofillers is calculated based on this equation (Table 4). Besides, experimental δ was obtained by analyzing the Fig. 5b-d and data summarized in Table 4. Results show that thickness of the layers between the MWCNTs is the lowest compared to the other nanofillers. Comparing the experimental and theoretical data, the same trend is observed but the quantities are lower for the experimental findings. Since the molecular weight of our TPU is 10^5 g/mol, the radius of gyration (R_g) of TPU is obtained in the range of 15 to 30 nm. It is clear from the results that $\delta \gg R_g$, so the thickness is large enough that the hard segments could microphase separate in the required time. FESEM images of the annealed TPU/MWCNTs above the percolation threshold are shown in Fig. 6. Once the samples annealed, microphase separated domains can be seen due to the hard segments assembly. It means that at the nanoscale

TABLE 3. Number of nanofillers and hard segments, total surface area of nanofillers, required surface area and excess required nanofillers of nanocomposites.

Sample	Number of nanofillers	Total surface area of nanofillers (nm^2)	Number of hard segment	required surface area (nm^2)	excess required nanofillers (g)
TPU/MWCNTs (0.1 wt%)	5×10^{14}	2.5×10^{19}	10^{21}	5×10^{20}	2.1
TPU/CBNPs (0.1 wt%)	5×10^{13}	10^{19}	10^{21}	5×10^{20}	4.9
TPU/HNTs (0.1 wt%)	1.6×10^{14}	1.005×10^{19}	10^{21}	5×10^{20}	4.8

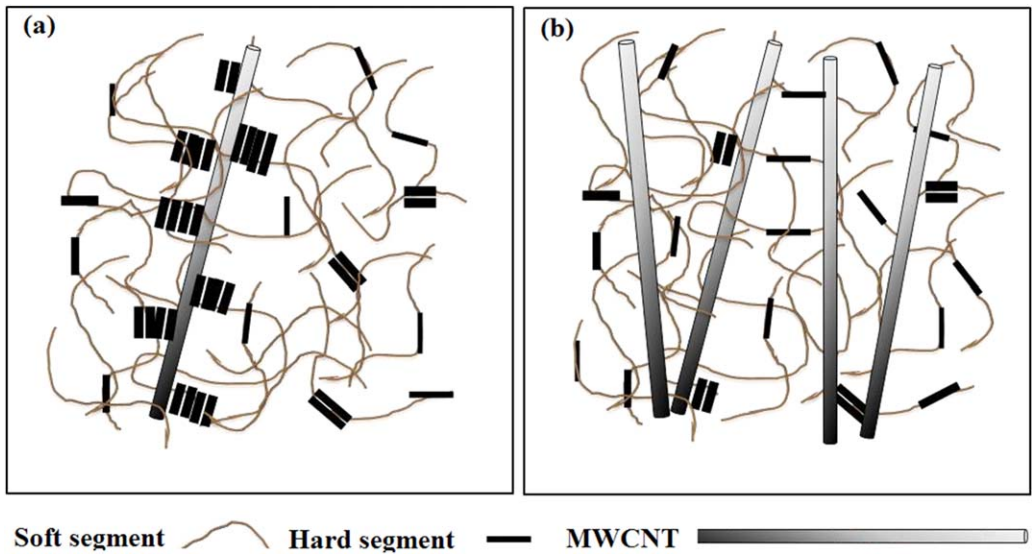

FIG. 4. Schematic representation for microphase separation of TPU nanocomposites containing (a) low and (b) high MWCNTs content. [Color figure can be viewed at wileyonlinelibrary.com]

level, the TPUs crystallize much slower than before, and the formation of ordered structures requires long experimental time scale.

To clarify that is there microphase separation above the percolation threshold or not, some tests using RMS analysis were defined. First, MWCNTs nanocomposite

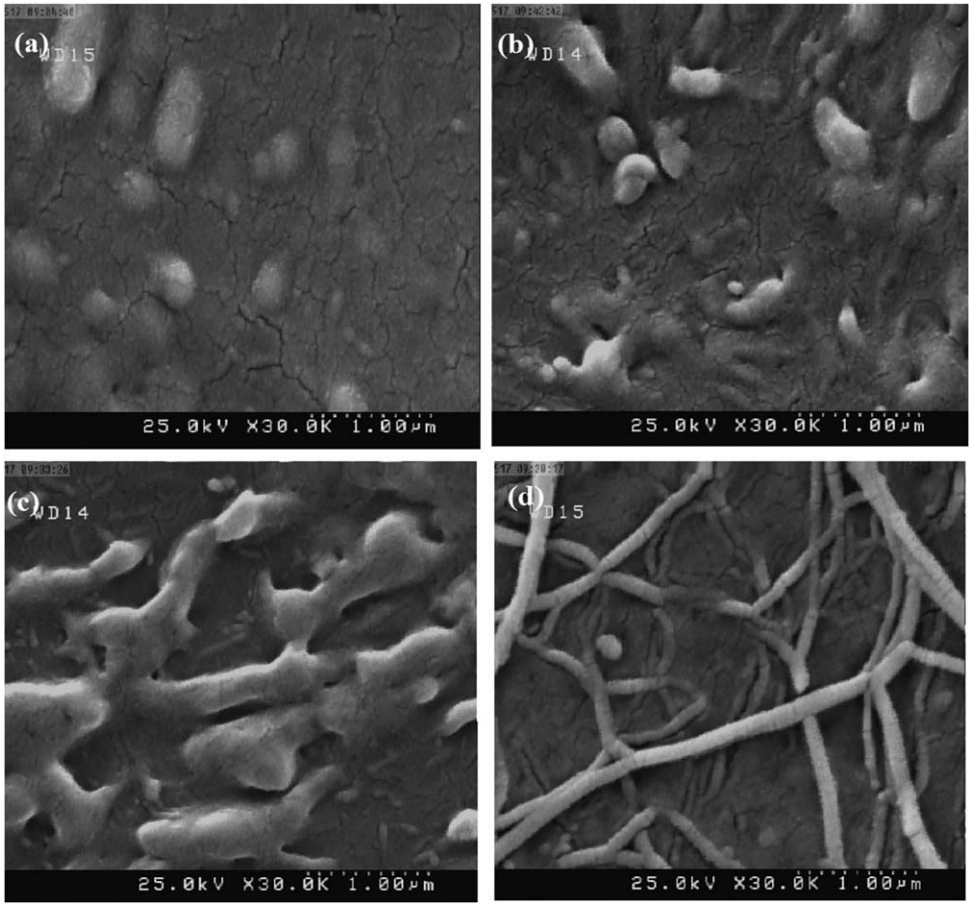

FIG. 5. FESEM images of quenched samples (a) neat TPU, (b) TPU/CBNPs, (c) TPU/HNTs and (d) TPU/MWCNTs (Above the percolation threshold).

 DOI 10.1002/pc

TABLE 4. Theoretical and experimental δ of nanocomposites.

Sample	Mass of the nanofillers (g)	Aspect ratio	Theoretical δ (nm)	Experimental δ (nm)
TPU/MWCNTs	0.8	225	250	273
TPU/HNTs	2	65	346	375
TPU/CBNPs	5	10	900	540

was melted at 210°C then they were cooled quickly to the microphase separation temperature (150°C). It is worthy to mention that two types of cooling process were used. Some samples were quenched and others were annealed after cooling down to 150°C for 2 h. Finally, the temperature sweep test was used. As seen from Fig. 7a-b, the storage and loss modulus belong to the annealed sample are 1.000 times higher than quenched one. This increment could be related to formation of the microphase separated domains. A question is arisen that the increase in the modulus only is related to the microphase separation of the hard and soft segments or also nanofillers have a role on that. For this purpose, time sweep test with a preshear (15 s^{-1}) was used at 190°C. It is important to mention

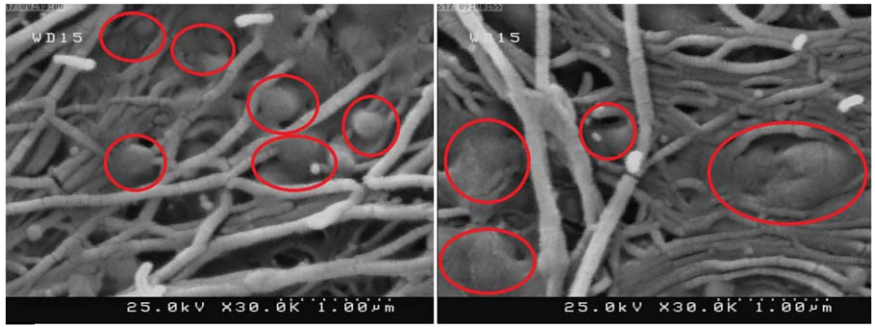

FIG. 6. FESEM images of annealed TPU/MWCNTs (Above the percolation threshold). [Color figure can be viewed at wileyonlinelibrary.com]

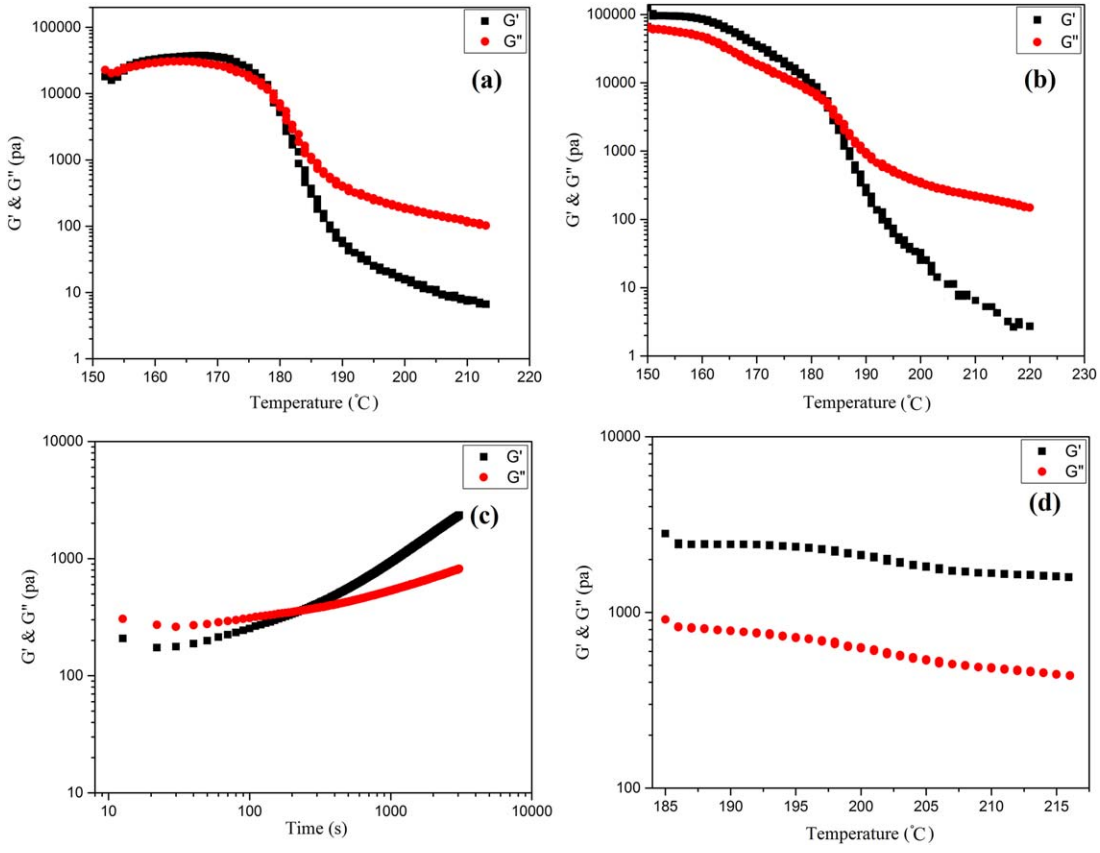

FIG. 7. Temperature sweep test of (a) quenched and (b) annealed TPU/MWCNTs above the percolation threshold at 150°C. (c) Time sweep test of annealed TPU/MWCNTs above the percolation threshold at 190°C. (d) Temperature sweep test of annealed TPU/MWCNTs above the percolation threshold at 190°C. [Color figure can be viewed at wileyonlinelibrary.com]

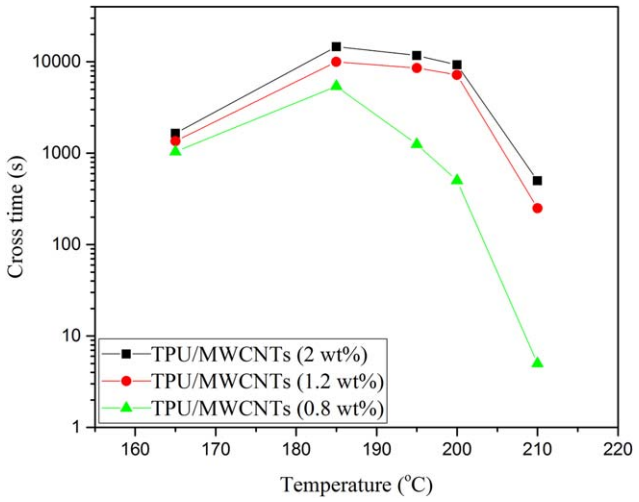

FIG. 8. Cross time as function of temperature for three MWCNTs nanocomposites above the percolation threshold. [Color figure can be viewed at wileyonlinelibrary.com]

that due to the sample homogeneity at this temperature, microphase separation cannot happen. After time sweep test, temperature sweep test was used. It is clear from Fig. 7c-d that no significant increase in the modulus is found, indicating that the former increment is just related to the formation of microphase separated domains even above the percolation threshold.

Various factors like filler-filler interactions, hydrodynamic forces, reorientation of anisometric nanofillers, and Brownian motion affect the reagglomeration of nanofillers and reconstruction of the filler network. Below the percolation threshold, the interaction between nanofillers does not have a great influence. However, as the nanofiller concentrations are enhanced, the mentioned factor becomes more important. Brownian motion is affected by temperature. At higher temperatures, due to the decrease in viscosity, role of Brownian motion will be enhanced for the reorganization of the percolation network. In TPU nanocomposites, there is a competition between reagglomeration of nanofillers and formation of microphase separated domains and both processes affect the final morphology and properties of the nanocomposites. Figure 8 shows cross time as function of temperature for three MWCNTs nanocomposites above the percolation threshold. It is worthy to mention that prior to the time sweep test; the samples were exposed to shear (15 s^{-1}) to break down the initial structure. The results show that at first, a surge in temperature increases the cross time and then decreases it. The maximum cross time corresponds to 185°C for all samples. At high temperatures, due to decrease in viscosity and increase in diffusivity, reagglomeration of nanotubes happens in shorter time spans. On the other hand, at low temperatures, hard segments assembly helps the reagglomeration of nanotubes and consequently the cross time is lower at microphase separation temperature range. Cross time as function of shear rate for three MWCNTs nanocomposites above the percolation threshold is shown in Fig. 9. At low shear rates, solid like behavior is observed and the increase in shear rate enhances the cross time (low shear rate has no ability to break the network structure). However, at high shear rates, the decrease in the cross time is observed. The reason is that at high shear rate, secondary aggregation of the nanotubes could be happened.

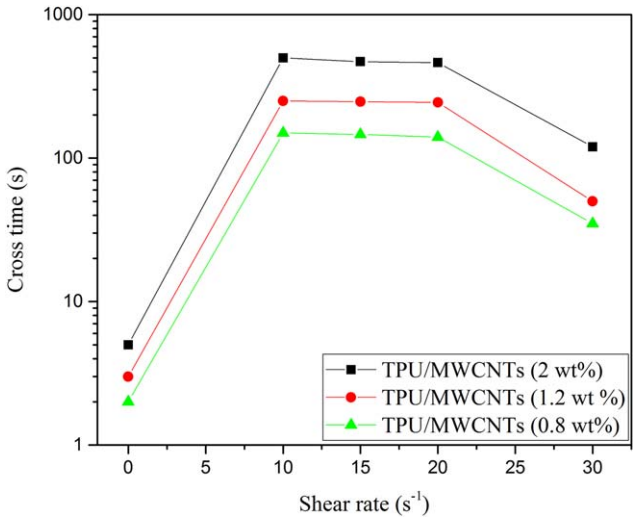

FIG. 9. Cross time as function of shear rate for three MWCNTs nanocomposites above the percolation threshold. [Color figure can be viewed at wileyonlinelibrary.com]

CONCLUSIONS

In current research, the effect of physiochemical characteristics of the nanofillers like aspect ratio, content and affinity to interact with hard and soft segments on the microphase separation kinetics of TPU nanocomposites has been investigated. For this purpose, TPU was synthesized and melt-compounded with three kinds of nanofiller, i.e. multi-walled carbon nanotubes, Closite 30B nanoplates and halloysite nanotubes. Spectroscopy results showed that degree of microphase separation of the samples containing 0.1 wt% nanofiller is higher than the nanocomposites above the percolation threshold. RMS and DSC analysis showed that the maximum of nucleation efficiency belongs to the MWCNTs; because the MWCNTs have the outstanding ability to absorb hard segments via noncovalent π- π interactions. The Avrami parameters, obtained by rheological results revealed that by incorporating nanofillers into TPU matrix, half crystallization time decreases strongly compared with the neat TPU. Time sweep tests showed that at 0.1 wt% nanofillers content, the nanocomposites have the fastest microphase separation kinetics. When the nanofiller content is enhanced, the distance between close nanofillers is decreased and therefore prevents the hard segment microphase separation. It is obvious from FESEM images that microphase separated domains do not exist for quenched samples above percolation threshold due to agglomeration

DOI 10.1002/pc

of nanofillers, although once the samples annealed, microphase separated domains can be seen due to the hard segments assembly even under confinement. Finally, temperature and shear rate have similar effect on the cross time of TPUs/MWCNTs nanocomposites above percolation threshold and cross time versus both temperature and shear rate is a bell-shaped curve.

REFERENCES

1. G. Oertel, L. Abele, *Polyurethane Handbook: Chemistry, Raw Materials, Processing, Application, Properties*, Hanser Publishers, Germany (1985).
2. E. Shahrousvand, M. Shahrousvand, M. Ghollasi, E. Seyedjafari, I.S. Jouibari, A. babaei, and A. Salimi, *Carbohydr. Polym.*, **171**, 281 (2017).
3. C. Sinturel, F.S. Bates, M.A. Hillmyer. *High χ–low N block polymers: how far can we go*? ACS Publications (2015).
4. S. Velankar, and S.L. Cooper, *Macromolecules*, **33**, 395 (2000).
5. Y. He, D. Xie, and X. Zhang, *J. Mater. Sci.*, **49**, 7339 (2014).
6. D. Pedrazzoli, and I. Manas-Zloczower, *Polymer*, **90**, 256 (2016).
7. S. Velankar, and S.L. Cooper, *Macromolecules*, **31**, 9181 (1998).
8. M.M. Mirhosseini, V. Haddadi-Asl, and S.S. Zargarian, *RSC Adv.*, **6**, 80564 (2016).
9. M. Shahrousvand, M.S. Hoseinian, M. Ghollasi, A. Karbalaeimahdi, A. Salimi, and F.A. Tabar, *Mater. Sci. Eng. C*, **74**, 556 (2017).
10. M. Shahrousvand, G.M.M. Sadeghi, E. Shahrousvand, M. Ghollasi, and A. Salimi, *Colloids Surf. B Biointerfaces*, **156**, 292 (2017).
11. M. D'Haese, P. Van Puyvelde, and F. Langouche, *Macromolecules*, **43**, 2933 (2010).
12. Y. Gupta, T. Bhave, A. Chakraborty, A. Pandey, R. Sharma, and D. Setua, *Polym. Eng. Sci.*, **56**, 1248 (2016).
13. M. Landa, J. Canales, M. Fernández, M.E. Muñoz, and A. Santamaría, *Polym. Test.*, **35**, 101 (2014).
14. S. Kango, S. Kalia, A. Celli, J. Njuguna, Y. Habibi, and R. Kumar, *Progr. Polym. Sci.*, **38**, 1232 (2013).
15. B. Finnigan, D. Martin, P. Halley, R. Truss, and K. Campbell, *J. Appl. Polym. Sci.*, **97**, 300 (2005).
16. A.J. Müller, M.L. Arnal, M. Trujillo, and A.T. Lorenzo, *Eur. Polym. J.*, **47**, 614 (2011).
17. D. Xu, and Z. Wang, *Polymer*, **49**, 330 (2008).
18. Z. Xu, Y. Niu, Z. Wang, H. Li, L. Yang, J. Qiu, and H. Wang, *ACS Appl. Mater. Interfaces*, **3**, 3744 (2011).
19. R.M. Michell, and A.J. Müller, *Progr. Polym. Sci.*, **54–55**, 183 (2016).
20. W. Zhao, Y. Su, X. Gao, J. Xu, and D. Wang, *J. Polym. Sci. Part B Polym. Phys.*, **54**, 414 (2016).
21. R.H. Lohwasser, G. Gupta, P. Kohn, M. Sommer, A.S. Lang, T. Thurn-Albrecht, and M. Thelakkat, *Macromolecules*, **46**, 4403 (2013).
22. Y. Huang, S. Ahir, and E. Terentjev, *Phys. Rev. B*, **73**, 125422 (2006).
23. I. Sahebi Jouibari, M. Kamkar, and H. Nazokdast, *Polym. Compos.*, DOI: 10.1002/pc.24563 (2017).
24. B. Fillon, B. Lotz, A. Thierry, and J. Wittmann, *J. Polym. Sci. Part B Polym. Phys.*, **31**, 1395 (1993).
25. D. Baskaran, J.W. Mays, and M.S. Bratcher, *Chem. Mater.*, **17**, 3389 (2005).
26. M. Amrollahi, and G. Sadeghi, *J. Appl. Polym. Sci.*, **110**, 3538 (2008).
27. Y.S. Lipatov, A. Nesterov, T. Ignatova, and D. Nesterov, *Polymer*, **43**, 875 (2002).